Received: 1 July 2018 | Accepted: 30 October 2018

DOI: 10.1113/EP087217

RESEARCH PAPER

WILEY EP Experimental Physiology

Identification and expression analysis of type II and type III P_i transporters in the opossum kidney cell line

Natalia Guillén[1] | Yupanqui A. Caldas[1,2] | Moshe Levi[2,3] | Víctor Sorribas[1]

[1]Department of Toxicology, University of Zaragoza, Zaragoza, Spain

[2]Division of Renal Diseases and Hypertension, Department of Medicine, University of Colorado Denver, Aurora, CO, USA

[3]Department of Biochemistry and Molecular and Cellular Biology, Georgetown University, Washington, DC, USA

Correspondence
Víctor Sorribas, University of Zaragoza, Veterinary Faculty, Department of Toxicology, Calle Miguel Servet 177, Zaragoza E50013, Spain.
Email: sorribas@unizar.es

Funding information
This work was supported by a grant from the Ministry of Economy and Competitiveness, code SAF2015-66705-P, and a grant from the Gobierno de Aragón and FSE 'Construyendo Europa desde Aragón', code B39_17R, both to V.S.

Edited by: Kate Denton

Abstract

The apical membrane of renal proximal tubular epithelial cells is the main controller of phosphate homeostasis, because it determines the rate of urinary P_i excretion. The opossum kidney (OK) cell line is a good model for studying this function, but only NaPiIIa (NaPi4) has been identified to date as a P_i transporter in this cell line. In this work, we have identified three additional P_i transporters that are present in OK cells: NaPiIIc, PiT1 and PiT2. All three sequences are similar to the corresponding orthologues, but PiT1 is missing the first transmembrane domain. Confluent cells exhibit characteristics of type II P_i transport, which increases with alkalinity and is inhibited by phosphonoformic acid (PFA), and they mainly express NaPiIIa and NaPiIIc, with a low abundance of PiT1 and PiT2. Proliferating cells show a higher expression of PiT1 and PiT2 and a low expression of NaPiIIa and NaPiIIc. Adaptation to a low P_i concentration for 24 h induces the expression of RNA from NaPiIIa and NaPiIIc, which is not prevented by actinomycin D. Small interfering RNA transfections revealed that PiT1 is not necessary for P_i transport, but it is necessary for adaptation to a low P_i, similar to NaPiIIa and PiT2. Our study reveals the complexity of the coordination between the four P_i transporters, the variability of RNA expression according to confluence and the heterogeneous correlation between P_i transport and RNA levels.

KEYWORDS
cloning, OK cells, P_i transporter

1 | INTRODUCTION

Inorganic phosphate homeostasis is achieved through the coordinated activity of intestinal absorption, bone storage and the renal excretion of surplus P_i (for reviews, see Biber, Hernando, & Forster, 2013; Chang & Anderson, 2017; Marks, Debnam, & Unwin, 2010). These three processes are the targets of a number of hormonal and non-hormonal regulatory mechanisms, which apparently act in a redundant manner. The evolutionary cost of the existence of so many regulatory mechanisms is justified not only by the physiological relevance of inorganic phosphate but also by the dangerous outcomes of P_i homeostasis dysregulation and toxicity (e.g. Chang & Anderson, 2017; Komaba & Fukugawa, 2016).

Of the aforementioned three processes, renal reabsorption/urinary excretion of P_i is recognized as the main and fastest mechanism for achieving phosphate homeostasis, and it is a target of all regulators known to affect P_i homeostasis. Most renal P_i reabsorption takes place in the proximal tubule through the activity of sodium-coupled P_i cotransporters expressed in the apical membrane of the epithelial cells. Two type II P_i transporters, NaPiIIa and NaPiIIc (Forster & Werner, 2018; Forster, Hernando, Biber, & Murer, 2013), and two type III P_i transporters, PiT1 and PiT2 (Forster et al., 2013; Sorribas, 2018), are expressed in the proximal tubule. However, only NaPiIIa, NaPiIIc and PiT2 have been described in the apical brush-border membrane, and they are regulated by dietary P_i deprivation in different ways (Villa-Bellosta et al., 2009b). Therefore, in addition to the activity of many regulatory mechanisms, the presence of several P_i transporters that are not regulated in a similar manner further complicates our ability to understand this important homeostatic function precisely.

For study of the cellular and molecular mechanisms of P_i reabsorption, the most common *in vitro* model is the opossum kidney (OK) cell line. In this line, factors such as the kinetic characteristics of P_i transport (including the response to pH changes), the regulation by parathyroid hormone and the P_i concentration in the culture medium, and the expression of NaPiIIa are similar to the responses and characteristics observed in the proximal tubule (e.g. Malmström & Murer, 1986; Sorribas et al., 1994). Nevertheless, although OK cells have helped us to understand some of the molecular mechanisms of

NaPiIIa regulation, they represent a limited cell model, both because this model lacks a genome sequence of the original species (*Didelphis virginiana*) and because of the scarcity of commercial antibodies. In this respect, the various groups that are working in this area have been unable to generate functional and valid antibodies against the endogenous NaPiIIa (formerly NaPi4). One exception is Professor Lederer's group, which was able to generate a functional polyclonal antibody (Lederer, Sohi, Mathiesen, & Klein, 1998).

In this work, we have attempted to overcome the aforementioned limitations regarding the use of OK cells when studying renal tubular proximal P_i transport. Although the only P_i transporter that had been identified and sequenced in these cells up to now was NaPiIIa (Sorribas et al., 1994), we have now been able to sequence the three other types of sodium-coupled P_i transporters in the kidney known to date: NaPiIIc, PiT1 and PiT2. Sequences were analysed *in silico* for two-dimensional (2D) modelling, and the various expressions of the four transporters were also studied as a function of culture confluence and the concentration of P_i in the medium. The expressions were contrasted with the characteristics of the resulting transport, in combination with RNA interference, subsequently leading us to reach conclusions about the relevance of each transporter in the total P_i uptake by these cells.

New Findings

- **What is the central question of this study?**
  The opossum kidney (OK) cell line is the main *in vitro* model of proximal tubular P_i transport, but it is incomplete because only the NaPiIIa P_i transporter has been identified.
- **What is the main finding and its importance?**
  We have cloned and characterized the P_i transporters NaPiIIc, PiT1 and PiT2 from OK cells and have analysed the relevance of the four transporters to P_i transport. All four transporters are involved in the upregulated P_i transport of cells incubated using a low-P_i medium, and only PiT1 is not involved in basal transport.

2 | METHODS

2.1 | Cell culture and transport assays

Opossum kidney proximal tubule (OK) cells, a permanent cell line originally obtained from a female American opossum kidney (Koyama, Goodpasture, Miller, Teplitz, & Riggs, 1978), were grown in Dulbecco's modified Eagle's medium (DMEM)–Ham's F12 supplemented with 10% fetal calf serum (FCS), penicillin, streptomycin and L-glutamine at 37°C in air supplemented with 5% CO_2. At confluency, cells were made quiescent by incubating them in the same medium with FCS at 0.2% for 24 h. For various P_i concentrations in the culture media, P_i-free DMEM with 0.2% FCS was used, which was ultimately supplemented with 0.1, 1 or 2 mmol l^{-1} P_i (from a combination of K_2HPO_4 and KH_2PO_4 for a final pH of 7.4). All culture reagents were from Gibco (Thermofisher Scientific, Waltham, MA, USA).

Transport assays were performed on plastic support, as described (Sorribas et al., 1994; Villa-Bellosta & Sorribas, 2009). ^{32}P-H_2PO_4 was used as a radiotracer at 5 μCi ml^{-1} in uptake media (PerkinElmer, Waltham, MA, USA).

2.2 | Rapid amplification of complementary DNA ends (RACE)

For the identification and subsequent sequencing of OK cell complementary DNA (cDNA), we used an RNA ligase-mediated, rapid amplification procedure of 5′ and 3′ ends of cDNA with a GeneRacer kit from Invitrogen (Thermofisher Scientific), following the manufacturer's instructions. For amplification, gene-specific primers were designed from a consensus region of aligned sequences of *Monodelphis domestica*, *Mus musculus*, *Rattus norvergicus* and *Homo sapiens* to generate overlapping 5′ and 3′ ends of cDNA. The sequence analysis and assembling were carried out using MacVector v.14.0 (MacVector, Inc, Cary, NC, USA). The sequences of NaPiIIc, PiT1 and PiT2 obtained from *Didelphis virginiana* were reported to GenBank (http://www.ncbi.nlm.nih.gov/Genbank/index.html) with the accession numbers MH397475, MH397476 and MH397477, respectively.

2.3 | Pharmacological treatments

All chemicals were from Sigma-Aldrich (St Louis, MO, USA). Quiescent OK-P cells were incubated for 24 h in the presence or absence of either 1 μmol l^{-1} actinomycin D or 0.01 μmol l^{-1} triiodo-L-thyronine (T_3) and different concentrations of P_i. Reagents were dissolved in dimethyl sulfoxide (DMSO), and the same amount of solvent was added to the control cells (0.1% final concentration; i.e. 1:1000 dilution).

2.4 | RNA interference

All reagents for RNA interference and transfection were from Ambion (Thermofisher Scientific). Validated small interfering RNAs (Silencer Select siRNAs) were transfected using a final concentration of 10 nmol l^{-1} according to the manufacturer's instructions. Cells were incubated for 24 h with Lipofectamine RNAiMAX, and the corresponding RNAis in OPTIMEM. Subsequently, the medium was replaced with DMEM–F12, supplemented with 10% FCS, and the cells were incubated for an additional 48 h until the corresponding assay was performed. Real-time PCR revealed that maximal reduction of the target RNAs in OK cells was observed after 48 h. A scrambled siRNA with a similar base composition was used as a negative control.

2.5 | Real-time PCR

Total RNA was purified from OK cells using Quick-RNA MiniPrep (Zymo Research, Irvine, CA, USA), and it was treated with DNase I. Total RNA was retrotranscribed using a PrimeScript RT Reagent Kit (Perfect Real Time) (Takara Bio Inc., Kusatsu, Japan) and amplified in a

TABLE 1 Primers used in qPCR

Gene name	Protein name	Accession	Sequences	Amplicon size (bp)
SLC34A1	NaPi-IIa (NaPi4)	L26308	CTTGTCTAATCCTGTGGCTGGT ATGCTGACGATGATGGAGGTAG	93
SLC34A3	NaPi-IIc	XM_007475446	GCTCTGGAAAAACTCAGTGGTC TCTAGCTGCACAATGAGATGGG	119
SLC20A1	PiT-1	XM_007477571.1	TTCTGTTGTACGGTGGCGTT ATGCAATGACTACGGTGAGAGC	150
SLC20A2	PiT-2	XM_007476411.1	GGGGCACCAGTATTAGGTTTGA TCTTGATAGGGCACCCTCTTTC	159
GADPH	GADPH	DQ403044	TCCTGCACTACCAACTGCTT AAGCAGGGATGATATTCTGGGC	177
BETA-ACTIN	β-actin	AY944136	AAGAAATCACAGCCCTGGCA GAAGCCAGAATAGAGCCACCAA	100

LightCycler 1.5 (Roche, Mannheim, Germany) using a SYBR Premix Ex Taq II (Takara). The primers used are shown in Table 1. Gene expression data were normalized to an endogenous reference (*GADPH*) and to a calibrator according to the manufacturer's instructions.

2.6 | Cell membrane preparation and immunoblot analysis

After treatments, cells grown in 100 mm dishes were scraped into 5 ml of ice-cold PBS and centrifuged at 15000g for 10 minutes. The cell pellet was resuspended in 1 ml of buffer [20 mmol l^{-1} Tris–HCl (pH 7.5), 2 mmol l^{-1} $MgCl_2$, 250 mmol l^{-1} sucrose and proteinase inhibitors; Roche Diagnostics] and was kept on ice for 15 min. Cells were then passed through a 22-gauge needle 20 times, and the cell debris was separated by centrifugation at 1000*g* for 10 min at 4°C. The supernatant was recentrifuged at 30,000*g* for 90 min at 4°C, and the cell membrane pellet was resuspended in 100 μl of lysis buffer [50 mmol l^{-1} Tris–HCl (pH 8.0), 80 mmol l^{-1} NaCl, 2 mmol l^{-1} $CaCl_2$ and 1% Triton X-100 or 1% CHAPS], with the same proteinase inhibitors.

The protein concentration was determined using a BCA kit (Pierce, Thermofisher Scientific). Twenty-five micrograms of protein were separated by SDS-PAGE at 10% for 150 min at 100 V in a Miniprotean cell (Bio-Rad, Hercules, CA, USA). Proteins were transferred electrophoretically onto polyvinylidene difluoride membranes (Bio-Rad) using a Trans-Blot Turbo Transfer System (Bio-Rad) according to the manufacturer's instructions. Membranes were incubated overnight with the primary antibodies at 4°C. After incubation with a secondary antibody linked to horseradish peroxidase, the reaction was developed using the Luminata Crescendo (Millipore, Billerica, MA, USA), and the image was captured and analysed using the Versadoc Image System (Bio-Rad).

Polyclonal antibodies were prepared in rabbits by injecting peptides conjugated to keyhole limpet haemocyanin and mixed in Freund's complete adjuvant (Davids Biotechnologie, Regensburg, Germany). The following peptides were used:

(i) NaPiIIc: SPDQEEEGEADPWALPQLKTS. The sequence corresponds to amino acids 39–59, which are located in the intracellular compartment, before the first transmembrane domain.

(ii) PiT1: EKKSSLKEDHEEAKLSLGDGE, corresponding to amino acids 269–289, a peptide located at the beginning of the large, central intracellular loop [between transmembrane domains (TMDs) VI and VII].

(iii) PiT2: HKDSGLYKDLLHKIHLDRGPD, corresponding to amino acids 348–368, also located in the middle of the large, central intracellular loop.

None of these antibodies provided reliable specific signals, either after the quality controls with pre-immune serum and peptide blocking or after the optimizations with different dilutions and detergents. Therefore, no results are shown. However, for NaPiIIa (formerly, NaPi4), a polyclonal antibody was generously donated by Professor Eleanor Lederer (University of Louisville School of Medicine, KY, USA) and was used as a control for the indicated experiments.

2.7 | Statistics

All experiments were repeated three times, using triplicates per condition, and are shown as means ± SD. GraphPad Prism 5.0 (GraphPad Software, La Jolla, CA, USA) was used for statistical analysis. The significances of differences were determined by unpaired Student's *t* test or by one-way ANOVA with Tukey's *post hoc* test for multiple comparisons, depending on the experiment and the number of means. Differences were considered significant when the *P* values were < 0.05.

3 | RESULTS

3.1 | Cloning of PiT1, PiT2 and NaPiIIc from OK cells

RACE assays provided the complete coding region sequence of PiT1 (677 amino acids) and PiT2 (653 amino acids). In the case of NaPiIIc, only the 5′-RACE was obtained, which included the first 422 amino acids. A 2D model of PiT1 is shown in Figure 1a, with several common and uncommon characteristics revealed after an alignment with various orthologues. Common characteristics include a glycosylation

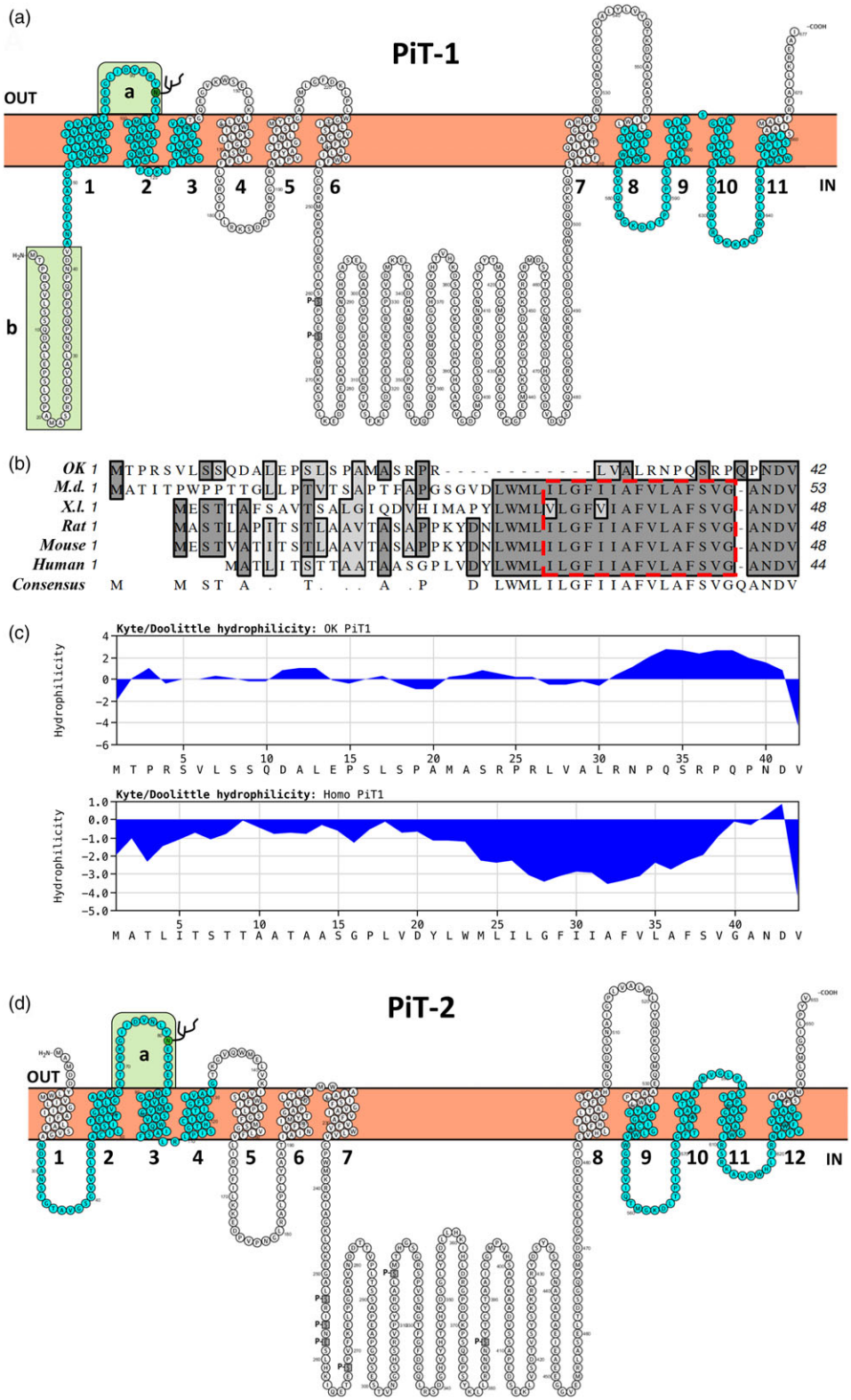

FIGURE 1 Structural two-dimensional model of PiT1 and PiT2 from opossum kidney (OK) cells. The complete amino acid sequences are shown. (a) PiT1 is outlined in an 11-transmembrane domain (TMD) model, beginning at an intracellular amino-terminus. The *N*-glycosylation site at N94 in the first extracellular loop and two phosphorylation sites at S261 and S265 in the large intracellular loop are also shown. Two phosphate transporter family domains, pfam01384 (PHO4), are shown in blue amino acid residues, encompassing amino acids 43–140 and 561–659. The extracellular region between TMDs 1 and 2 (a, in green box) contains several residues involved in P_i transport and affinity. (b) Alignment of the first 42 amino acids (b, also in green box) with the N-termini of several orthologues. The red dashed box indicates the first common TMD, which is not present in OK cells. (c) A hydropathy Kyte/Doolittle analysis of the first 42 amino acids of PiT1 from OK cells is shown and compared with the same terminus of the human orthologue, which reveals the high hydrophilicity of the OK amino-end sequence. (d) Two-dimensional model of PiT2, with the accepted 12 TMDs and both protein ends located extracellularly. All annotations are as for PiT1

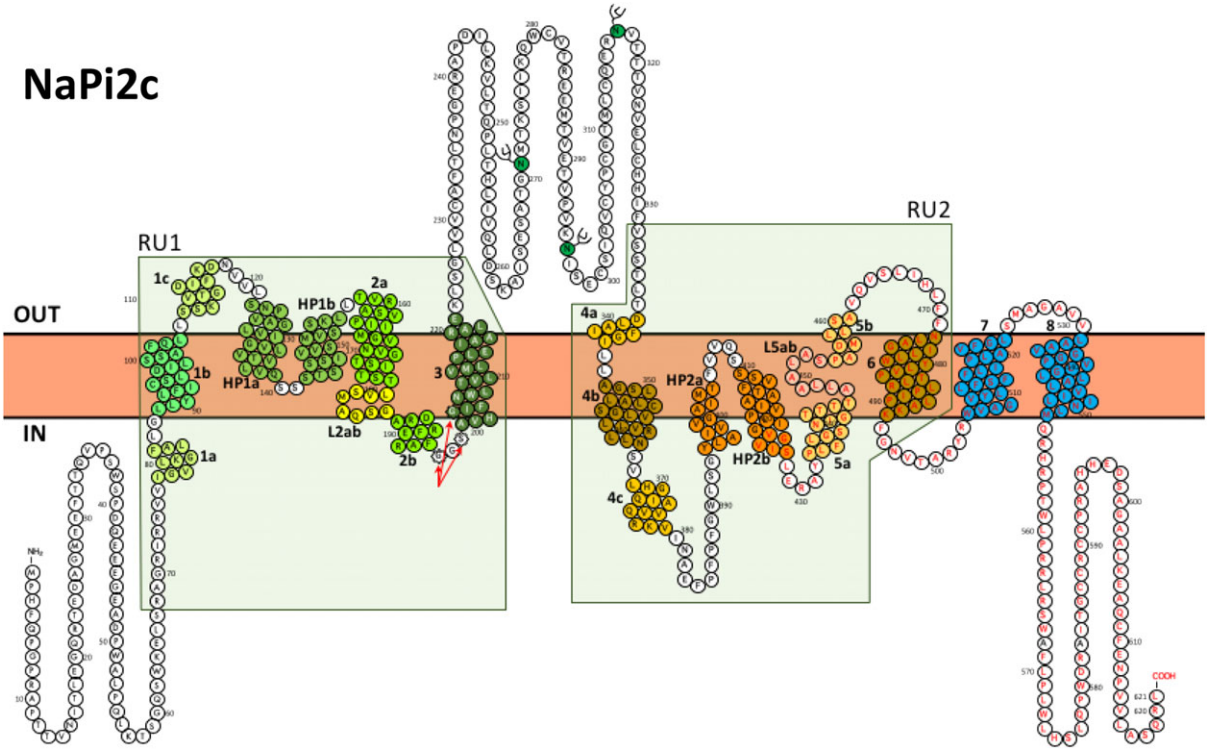

FIGURE 2 Structural two-dimensional model of NaPiIIc from OK cells. Given that only the first 422 amino acids were identified, purely for the purpose of modelling, the remaining amino acids, 423–621 (letters in red), were copied from *Monodelphis domesticus*. This two-dimensional model was developed from the proposed three-dimensional structure of NaPiIIa (Fenollar-Ferrer et al., 2014). RU1 and RU2 are repeated structural units that constitute the transport core of the protein. Proposed intra- or extramembrane helices are numbered from 1 to 8. Former re-entrant repeats are now depicted as hairpins 1a, 1b, 2a and 2b. Transmembrane helices 2 and 5 are divided by non-helical intramembrane loops L2ab and L5ab. The last two TMDs (7 and 8) are not a part of the repeated core. Red arrows indicate amino acids that determine the electrogenicity in Slc34 P_i transporters: GSG in electroneutral NaPiIIc and AAD in electrogenic NaPiIIa

site at asparagine N94 within the first extracellular loop (amino acids 83–96); two phosphorylation sites at S261 and S265 in the main intracellular loop; and two phosphate transporter family domains (pfam01384) at amino acids 43–140 and 561–659, respectively (PHO4; https://www.ncbi.nlm.nih.gov/Structure/cdd/cddsrv.cgi?uid=pfam01384). The first loop (amino acids 83–96) is a region involved in P_i affinity and, according to the results of a combination of the two-electrode voltage clamp and substituted cysteine accessibility methods, this region seems to form part of a hydrophilic pore where the substrates interact with specific amino acids (Ravera, Murer, & Forster, 2013).

A hydropathy analysis revealed an uncommon structure of 11 TMDs, with the amino end located intracellularly and the carboxy terminus located extracellularly. This contrasts with the established 12-TMD model, in which both ends of the protein are located extracellularly (Bøttger & Pedersen, 2011; Ravera et al., 2013). The 11-TMD proposal is attributable to the absence, in OK cell PiT1, of the first accepted TMD of the 12-TMD model, which has the consensus sequence ILGFIIAFVLAFSVG in the other orthologue proteins (Figure 1b). This figure also shows the alignment of the first 42 amino acids of OK PiT1 with several orthologues, in addition to a Kyte/Doolittle hydropathy analysis that compares those OK PiT1 amino acids and Homo PiT1 amino end sequences (Figure 1c). Seven other tests provided similar hydropathy profiles using MacVector software and protocols for hydrophilicity and hydrophobicity (not shown).

PiT2 from OK cells shows a more conserved structure, including the 12 TMDs and both ends located extracellularly, with *N*-glycosylation located at N81, six potential phosphorylation sites in the large intracellular loop and the two pfam01384 domains (Figure 1d).

For the 2D modelling of NaPiIIc, the sequence of the 422 amino acids identified with 5′-RACE was fused *in silico* to amino acids 423–621 from *M. domestica* (accession no. XP_007475507). The added sequence is shown as red residues in Figure 2. A hydropathy analysis of the resulting chimeric protein provided the classical 12-TMD model (Forster, Hernando, Biber, & Murer, 2012). A more recent work has suggested a very interesting three-dimensional (3D) model of NaPiIIa (Fenollar-Ferrer et al., 2014) based on hydropathic, fold homology with the Na^+-coupled dicarboxylate transporter from *Vibrio cholerae* (Mancusso, Gregorio, Liu, & Wang, 2012). We have not developed a 3D model for OK NaPiIIc because it is beyond the scope of this work and because our sequence of NaPiIIc is incomplete. Nevertheless, Figure 2 shows a combination of a 2D model of NaPiIIc with several modifications and characteristics derived from the 3D model of NaPiIIa (Fenollar-Ferrer et al., 2014). In this model, both the amino and carboxy ends are still located intracellularly, and a large, central extracellular loop containing three *N*-glycosylation sites divides the protein into two parts, each one containing a repeated structural unit (amino acids

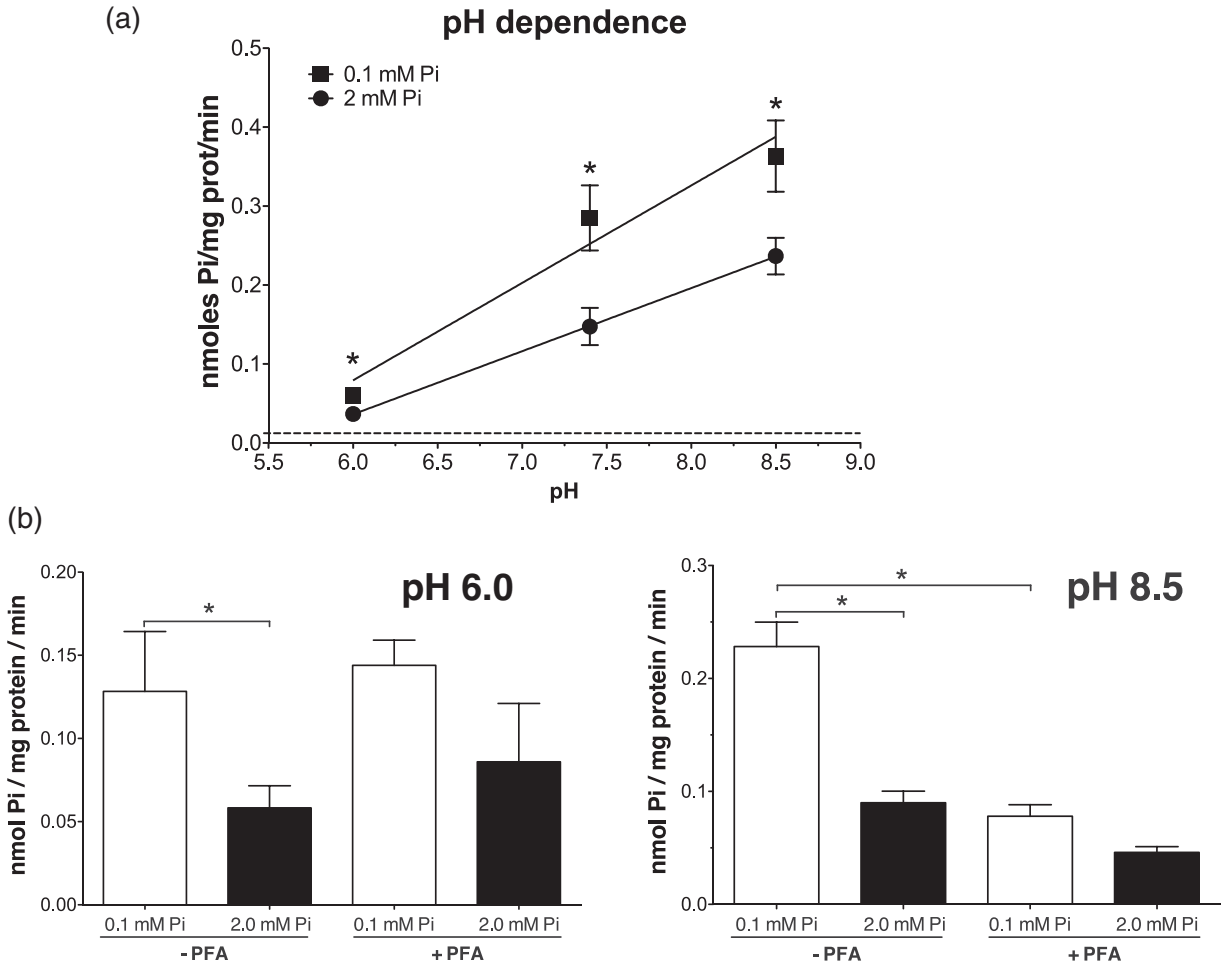

FIGURE 3 P_i transport in confluent OK cells. (a) P_i uptake in cells incubated for 24 h with either 0.1 or 2.0 mmol l^{-1} P_i, and as a function of pH. The pH dependence is shown with the corresponding regression lines for both P_i concentrations. The dashed line indicates the level of Na^+-independent uptake. Asterisks indicate significantly different means by unpaired Student's *t* test ($P < 0.05$). (b) Effect of 5 mM phosphonoformic acid (PFA) on total P_i uptake at either pH 6.0 or 8.5 in cells incubated as in (a). Asterisks indicate significantly different means by ANOVA and a multicomparison *post hoc* test ($P < 0.05$)

68–227 for RU1 and amino acids 332–496 for RU2, respectively). As in the case of NaPiIIa, these units would constitute the transport core of NaPiIIc. The model contains eight TMDs, with additional membrane domains now considered to be hairpins 1 (a,b) and 2 (a,b), which were formerly considered re-entrant repeats. Transmembrane domains 2 and 5 are complex structures, each one divided into two domains (a and b) by non-helical intramembrane loops L2ab and L5ab. Glycine 196, serine 198 and glycine 202, which mandate electroneutral activity in NaPiIIc and are respectively replaced in NaPiIIa by A, A and D to provide electrogenicity, are indicated by the three red arrows in RU1 (Patti, Ghezzi, & Forster, 2013). The last two complete TMDs, 7 and 8, mainly contribute to the 3D structure. The carboxy terminus of *M. domestica* also includes a binding site (SQRL) for PDZ domain-containing proteins, such as $NHERF3^{PDZK1}$ (Villa-Bellosta et al., 2008).

3.2 | Relevance of type II *versus* type III P_i transport

Beginning with a concentration of 1 mmol l^{-1} P_i, OK cells were incubated with 0.1 or 2 mmol l^{-1} P_i in DMEM for 24 h. Figure 3a shows that, as expected, the uptake of OK cells incubated with 0.1 mmol l^{-1} P_i was twice the uptake with 0.05 mmol l^{-1} $^{32}P_i$ at pH 7.4 compared with cells maintained in DMEM with 2 mmol l^{-1} P_i. The activity of the type II and III P_i transporters is very sensitive to the pH of the medium because they preferentially transport HPO_4^{2-} or $H_2PO_4^-$, respectively, and because the relative abundance of these P_i species is mainly dependent on the pH. In fact, at pH 7.5 monovalent P_i ($H_2PO_4^-$) is ~17%, whereas divalent P_i (HPO_4^{2-}) is ~83%. The effect of protons as competitors with the sodium binding sites has also been suggested (Hartmann et al., 1995). To study the uptake of each species more specifically, the same type of experiment was performed at pH 6.0 and 8.5, given that at pH 6.0, 86% of P_i is $H_2PO_4^-$, whereas at pH 8.5, 98% of P_i is HPO_4^{2-} (see Candeal, Caldas, Guillén, Levi, & Sorribas, 2017).

The uptake at pH 6.0 was approximately 20–40% of the uptake at pH 8.5, at either concentration of P_i, thereby showing the known preference of OK cells for divalent P_i (Figure 3a). To emphasize the linearity of the pH effect on P_i uptake, the regression lines of P_i uptake as a function of pH are also shown for both P_i concentrations, and they reveal no saturation at the pH range of the experiment. At all

three pH values, the uptake of 0.05 mmol l^{-1} $^{32}P_i$ was approximately double in cells adapted to 0.1 mmol l^{-1} P_i, compared with 2 mmol l^{-1} P_i. Given that type III P_i transporters (PiT1 and PiT2) have a preference for monovalent P_i and that type II P_i transporters (NaPiIIa and NaPi2c) have a preference for divalent P_i, the pH results suggest that in OK cells and our experimental conditions, type II activity is double that of type III at 0.05 mmol l^{-1} P_i. However, the results also show that the adaptation of type III P_i transport also takes place to the same extent as type II.

To confirm these conclusions and discard the presence of additional, unknown P_i transporters, we also used 5 mmol l^{-1} phosphonoformic acid (PFA) as an inhibitor of type II transporters (Figure 3b). At pH 6.0, the presence of PFA did not significantly inhibit P_i uptake, but at pH 8.5, PFA completely prevented adaptation to incubation with 0.1 mmol l^{-1} P_i for 24 h, and it maintained the uptake at the basal level of 2 mmol l^{-1} P_i.

3.3 | Basal mRNA expression of P_i transporters

The mRNA expression of the various P_i transporters was also assayed to test the predictions of the functional assays summarized in the preceding section. In basal conditions (i.e. 100% confluent OK cells grown in DMEM–F12 medium), NaPiIIa and NaPiIIc were the most abundant P_i transporters, and PiT2 was the least-expressed RNA (Figure 4a). This general expression pattern was maintained in cells incubated in P_i-deprived medium (0.1 mM) for 24 h, and it only showed an increased expression of NaPiIIa and NaPiIIc over type III transporters (see below). Before confluence (i.e. when the cells were proliferating), the most abundant transporter was always PiT1. Only when the cells were close to confluence (80%) did the expression of NaPiIIa and NaPiIIc begin to be significant. The results of the expressions at different confluent states are summarized in Figure 4b, where the expressions are represented on a logarithmic scale owing to the several-fold changes in expression as a function of culture confluence. This high variability in the expression of transporters with confluence should be considered to avoid any misinterpretation of the results.

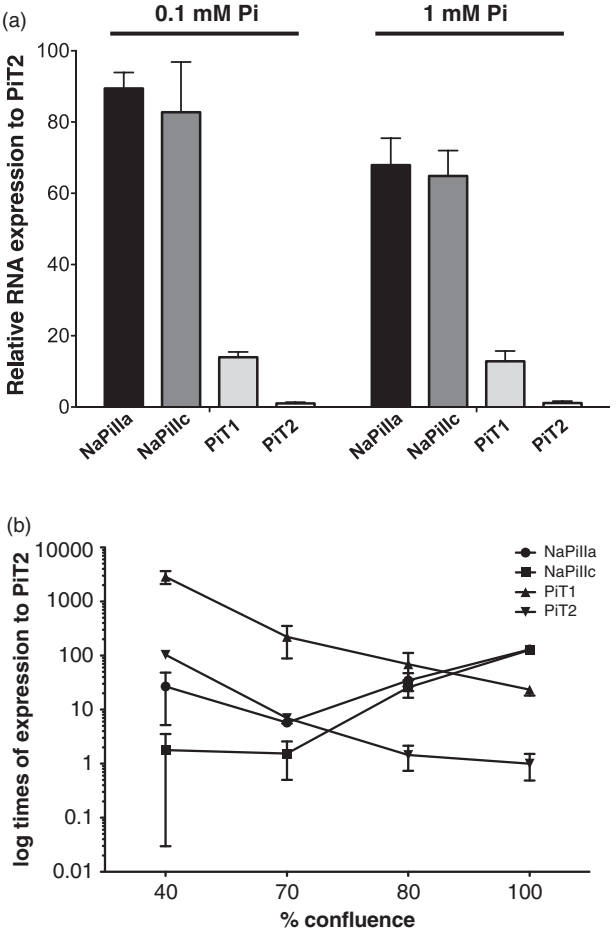

FIGURE 4 qPCR analysis of Na/P_i cotransporter RNA expressions in OK-P cells in relationship to PiT2, which is the least abundant P_i transporter. (a) Relative expressions in a culture at 100% confluence on a linear scale, in cells incubated for 24 h in 0.1 or 1 mM P_i. (b) Expressions of the P_i transporters with respect to PiT2 at the indicated percentages of confluence in cells grown in 1 mM P_i. A logarithmic scale on the ordinate axis is used owing to the high number of expression time differences. PiT1 and PiT2 expressions diminish and NaPiIIa and NaPiIIc expressions increase when the OK cell culture is more confluent

3.4 | Role of RNA transcription in P_i adaptation

Next, we analysed whether the adaptation to low P_i was dependent on changes in RNA transcription. The OK cells were incubated with either 0.1 or 2 mmol l^{-1} P_i for 24 h in the presence or absence of 1 μmol l^{-1} actinomycin D in DMSO (Figure 5). The same amount of solvent, with a final concentration of 0.1%, was added to the control cells. To avoid the repetition of previous reports, P_i transport activity was determined at the pH 6.0 and 8.5 to facilitate a study of the effects on type III and II P_i transport, respectively. Actinomycin D prevented the observed increase in P_i transport with 0.1 mmol l^{-1} P_i at pH 6.0 (i.e. when PiT1 and PiT2 are more active and relevant), therefore suggesting the dependence of these transporters on transcriptional activity. At pH 8.5, however, when HPO_4^{2-} and P_i uptake were at their highest, the adaptation persisted despite the treatment with actinomycin D, but transport activity was half the rate of cells without actinomycin D treatment, whether incubated at 0.1 or 2 mmol l^{-1} P_i.

3.5 | Changes in RNA abundance during adaptation to P_i concentrations in OK cells

To check whether the effects of actinomycin D on P_i transport were attributable, at least in part, to changes in the RNA abundance of any of the four transporters, the corresponding RNA levels were determined by real-time PCR (Figure 6a). The NaPiIIa RNA abundance increased in cells incubated with 0.1 mmol l^{-1} P_i, and this increase was resistant to actinomycin D; after 24 h of treatment, the abundance and adaptation effects were similar. The NaPiIIc RNA expression was also increased by low phosphate, and this increase was also resistant to actinomycin D. However, in the presence of the transcription inhibitor, actinomycin D, the expression of NaPiIIc RNA was reduced by half in cells maintained with either 0.1 or 2 mmol l^{-1} P_i.

We could not find clear and significant increased expressions of PiT1 or PiT2 RNAs. Nevertheless, these transcripts were the most

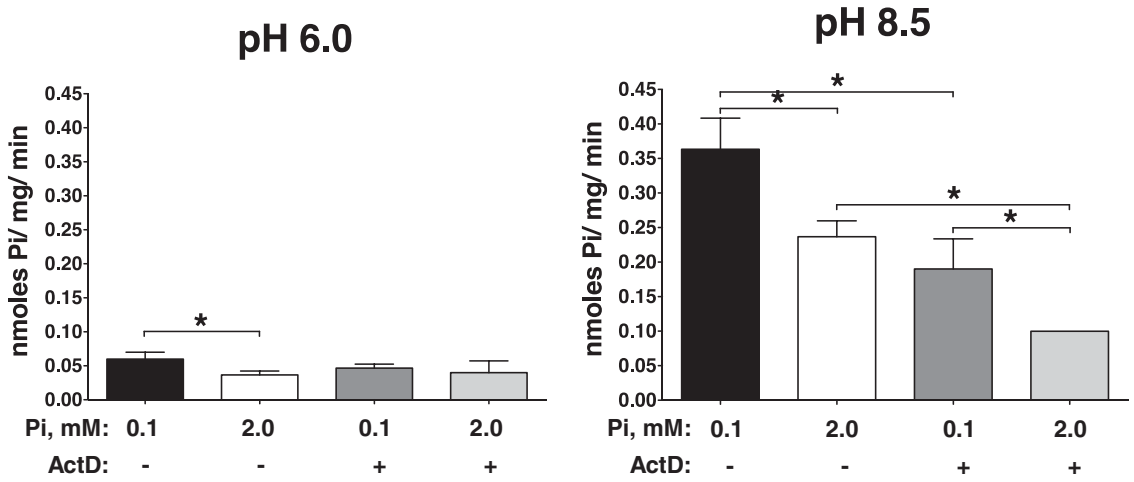

FIGURE 5 Effect of inhibition of transcription on adaptation to low and high (0.1 and 2 mmol l^{-1} P_i) phosphate concentrations at the indicated pH. Actinomycin D (ActD) prevents adaptation to low P_i when P_i transport is measured at pH 6.0. However, at pH 8.5 the effect of transcription inhibition on adaptation is not observed, although actinomycin D does reduce P_i uptake at both concentrations of P_i. Asterisks indicate significantly different means by ANOVA ($P < 0.05$)

sensitive to actinomycin D treatment; PiT1 expression was reduced by six times and PiT2 by 18 times.

Owing to the failure to obtain functional and reliable polyclonal antibodies (see Methods), we only used an anti-NaPiIIa antibody from OK cells donated by Professor Eleanor Lederer (Lederer et al., 1998). We checked the correlation between the RNA and the protein of NaPiIIa in cells that were incubated for 24 or 48 h with either 0.1 or 2 mmol l^{-1} P_i and actinomycin D (Figure 6b). At 24 h, actinomycin D did not clearly modify the expression of NaPiIIa. However, after 48 h the expression was reduced to one-third of the corresponding initial expression, at both 0.1 and 2 mmol l^{-1} P_i, and a modest adaptation persisted.

To confirm the accuracy of the determinations of RNA changes shown in Figure 6a, the abundances of the four P_i transporter RNAs were also measured after treating OK cells with 10 nmol l^{-1} triiodo-L-thyronine (T_3) for 24 h, as a positive control (Alcalde et al., 1999; Sorribas, Markovich, Verri, Biber, & Murer, 1995). Figure 6c shows that, in the case of NaPiIIa and NaPiIIc, T_3 induced 1.5 times the expression of each transporter, whereas PiT1 and PiT2 were unaffected in these cells.

3.6 | Specific relevance of P_i transporters in basal P_i transport in OK cells

Given that the effects of actinomycin D on P_i transport and the adaptation thereof can also be attributable to inhibiting the expression of many other proteins, such as regulators, receptors or scaffold proteins, we selectively inhibited the expression of transporters by using siRNAs (Figure 7). The efficiency of the interferences varied considerably among the experiments, ranging from 70 to >90% after 48 h (Figure 7a). The percentages of inhibitions were similar, despite the initial differences in transporter expressions. These expressions were similar whether they were transfected with scrambled siRNAs (Figure 7b) or were non-transfected (Figure 4; 100%). Even when the cells were transfected in a culture at 80% confluence, the cells were 100% confluent at the moment of the final assay owing to the necessary incubation of the cells for 48 h in DMEM–F12 supplemented with 10% FCS. This explains the difference between the RNA expressions of Figures 7b and 4b at 80% confluence.

The results of specific P_i transporter knockdown were absolutely unexpected. Functional assays after RNA interference were performed at different pH values to facilitate the interpretation of results. For PiT1 and PiT2 siRNA transfections, P_i transport was measured at pH 6.0 after 48 h, whereas for NaPiIIa and NaPiIIc, an uptake assay was performed at pH 8.5. Despite the higher expression of PiT1 over PiT2, siRNA inhibition of the expression of PiT1 did not cause any change in P_i transport (Figure 7c). However, RNA expression inhibition of PiT2 caused a 39% reduction in P_i transport, despite the lower expression of PiT2 compared with PiT1 and the other P_i transporters.

Regarding type II transporters, the results of inhibition were similar for both NaPiIIa and NaPiIIc (Figure 7d). P_i transport after NaPiIIa knockdown was reduced by 65%, whereas the interference with NaPiIIc resulted in a 59% reduction of P_i uptake. In the case of NaPiIIa, the inhibition of RNA expression with siRNA was accompanied by a reduction of protein expression, as confirmed by western blot (Figure 7e).

3.7 | Specific relevance of P_i transporters in OK cell adaptation

To ascertain the role of the various P_i transporters in adapting to a low or high P_i concentration in the culture medium, we transfected the cells (80% confluence) with the various siRNAs, and after 48 h, the cells were incubated with 0.1 or 2 mmol l^{-1} P_i for 24 h. The apparently unexpected results are shown in Figure 8. In all four cases, siRNA not only prevented adaptation to low P_i (0.1 mmol l^{-1}), but it also further reduced the uptake level in cells incubated with 2 mmol l^{-1} P_i. This reduction below the level of 2 mmol l^{-1} P_i was significant only in the case of NaPiIIa and NaPiIIc.

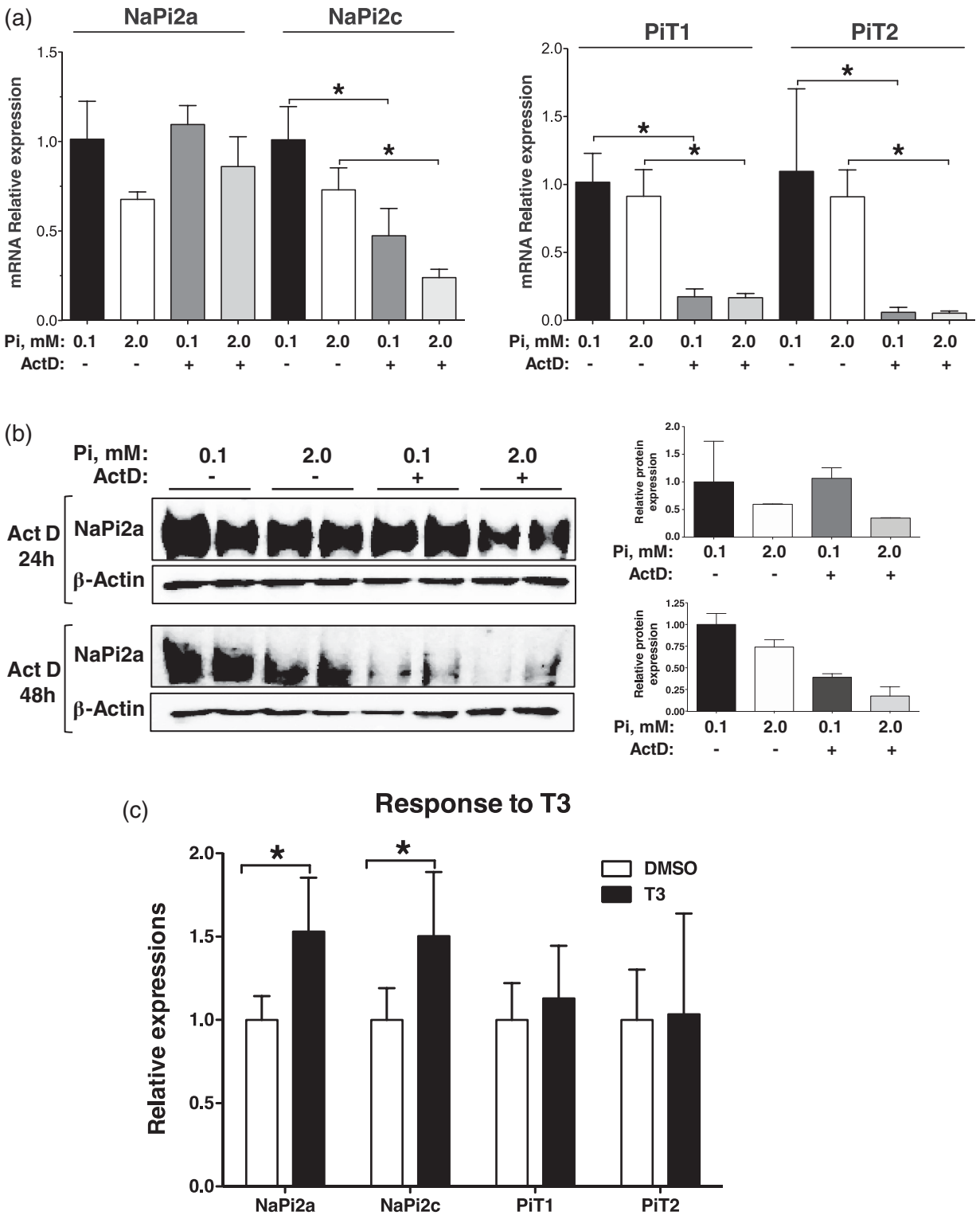

FIGURE 6 qPCR analysis of RNA Na/P_i transporter abundance in OK-P cells. (a) Effect on the abundance of the indicated Na/P_i cotransporter RNAs after 24 h of incubation with a low or high P_i concentration and with the transcription inhibitor actinomycin D (ActD). (b) Effect on NaPiIIa protein expression, in relationship to β-actin, in the same conditions as in (a), for 24 and 48 h. (c) Effect of 10 nM triiodo-L-thyronine (T_3) treatment for 24 h on the relative expression of P_i transporters. Asterisks indicate significantly different means by ANOVA ($P < 0.05$)

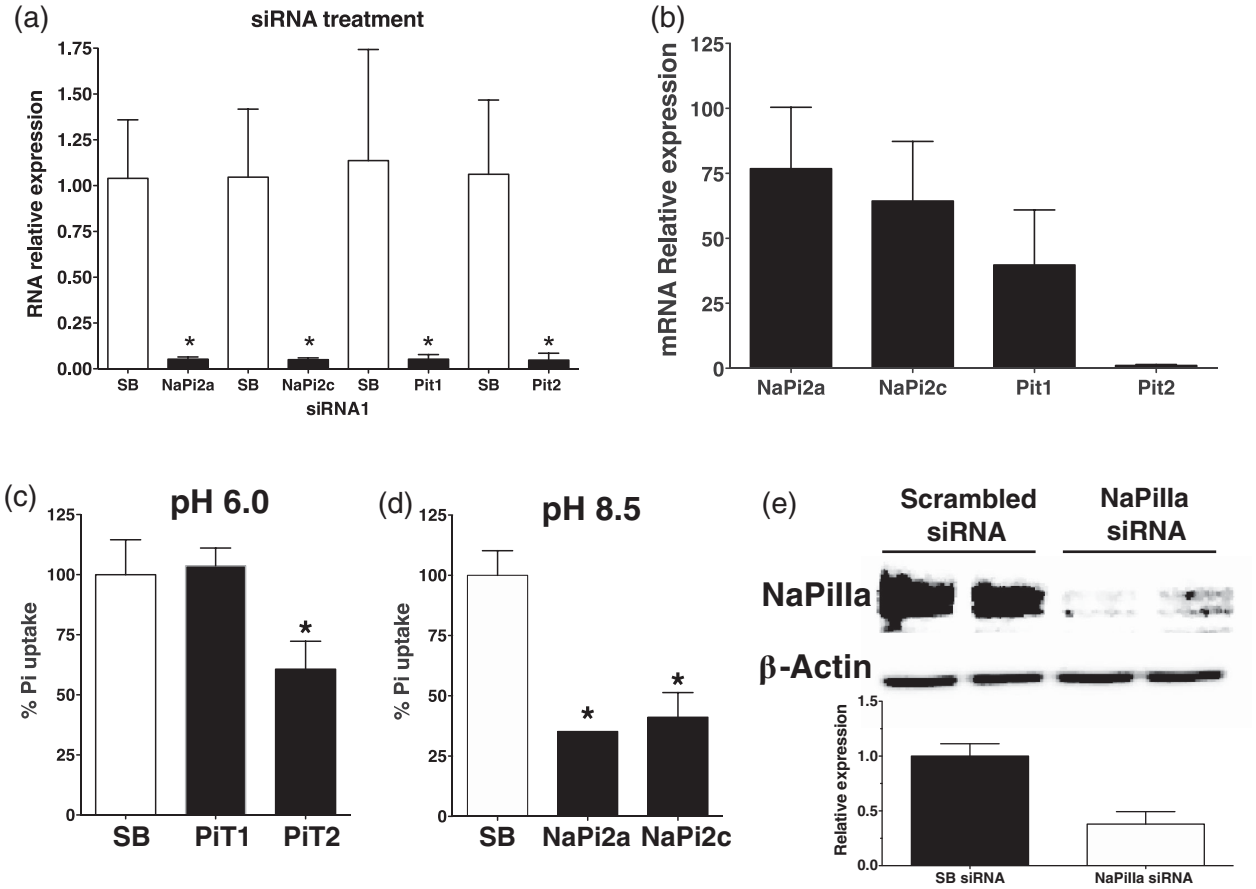

FIGURE 7 Effects of NaPiIIa, NaPiIIc, PiT1 and PiT2 RNA interference on specific RNA abundance and basal P_i uptake. (a) Efficiency of siRNA treatment on RNA abundance after 48 h of siRNA transfection against the indicated transporters using 80% confluent OK cells cultured in 1 mM P_i. Initial RNA abundances were as in Figure 3. (b) Relative expression of the four transporter RNAs after scrambled (SB) siRNA transfection. (c) Resulting P_i transport after 48 h of siRNA transfection with scrambled, PiT1 or PiT2 siRNAs. Transport was measured at pH 6.0 to maximize type III activity. (d) Resulting P_i transport after 48 h of siRNA transfection with scrambled, NaPiIIa or NaPiIIc siRNAs. The P_i transport was measured at pH 8.5 to maximize type II activity. (e) Immunoblot of NaPiIIa after 72 h of siRNA transfection. In all panels, asterisks indicate significant difference with an unpaired t-test from the corresponding scrambled siRNA transfection

4 | DISCUSSION

In this work, we provide new knowledge about the renal mechanisms of proximal tubular P_i transport, and the new findings can be divided into two main parts. First, we have identified the sequences of the missing P_i transporters in OK cells (NaPiIIc, PiT1 and PiT2), and second, we have studied the relevance of the various transporters to the total P_i uptake in OK cells and during adaptation.

Molecular identification was done by rapid amplification of cDNA ends. BLAST analyses of the amino acid sequences in combination with hydropathy algorithms revealed 2D structures similar to those accepted for the corresponding orthologues, with some exceptions. The main difference was related to PiT1, because the first 39 amino acids were very different with respect to the remaining orthologues, resulting in high hydrophilicity and low hydrophobicity of the amino-terminus, according to the hydropathy results (Figure 1c). Consequently, the first TMD of the accepted model of PiT1 in other species is not predicted for OK cell PiT1, and therefore, the model changes from 12 TMDs (Bøttger & Pedersen, 2011; Ravera et al., 2013) to 11 TMDs.

All the other characteristics present in PiT1 and PiT2 from OK cells have been described previously. This includes *N*-glycosylation and critical amino acids for P_i transport in the external region between TMDs 1 and 2 in PiT1 and TMDs 2 and 3 in PiT2 (Ravera et al., 2013), in addition to the two pfam01384 domains, the PD1131 homology domains (Salaün, Gyan, Rodrigues, & Heard, 2002) and the PiT signature sequences (Bøttger & Pedersen, 2011).

All three members of the type II family (*Slc34a1*, *Slc34a2* and *Slc34a3*) of P_i transporters also showed a similar primary structure, and with respect to the secondary structure, a 12-TMD 2D model has been consolidated over the years (for a review, see Forster et al., 2012). The OK NaPiIIc does not seem to be an exception, but this cannot be confirmed until the complete sequence is known, given that we identified only the first 422 amino acids (Figure 2). Merely for the purpose of representing the model, we combined this sequence fragment with the corresponding amino acids from the related marsupial, *M. domestica*. A hydropathy analysis of this chimeric sequence yielded the 12-TMD model, but instead of representing the model (any new knowledge would be insignificant), we decided to acknowledge the first 3D model of a member of the Slc34 family

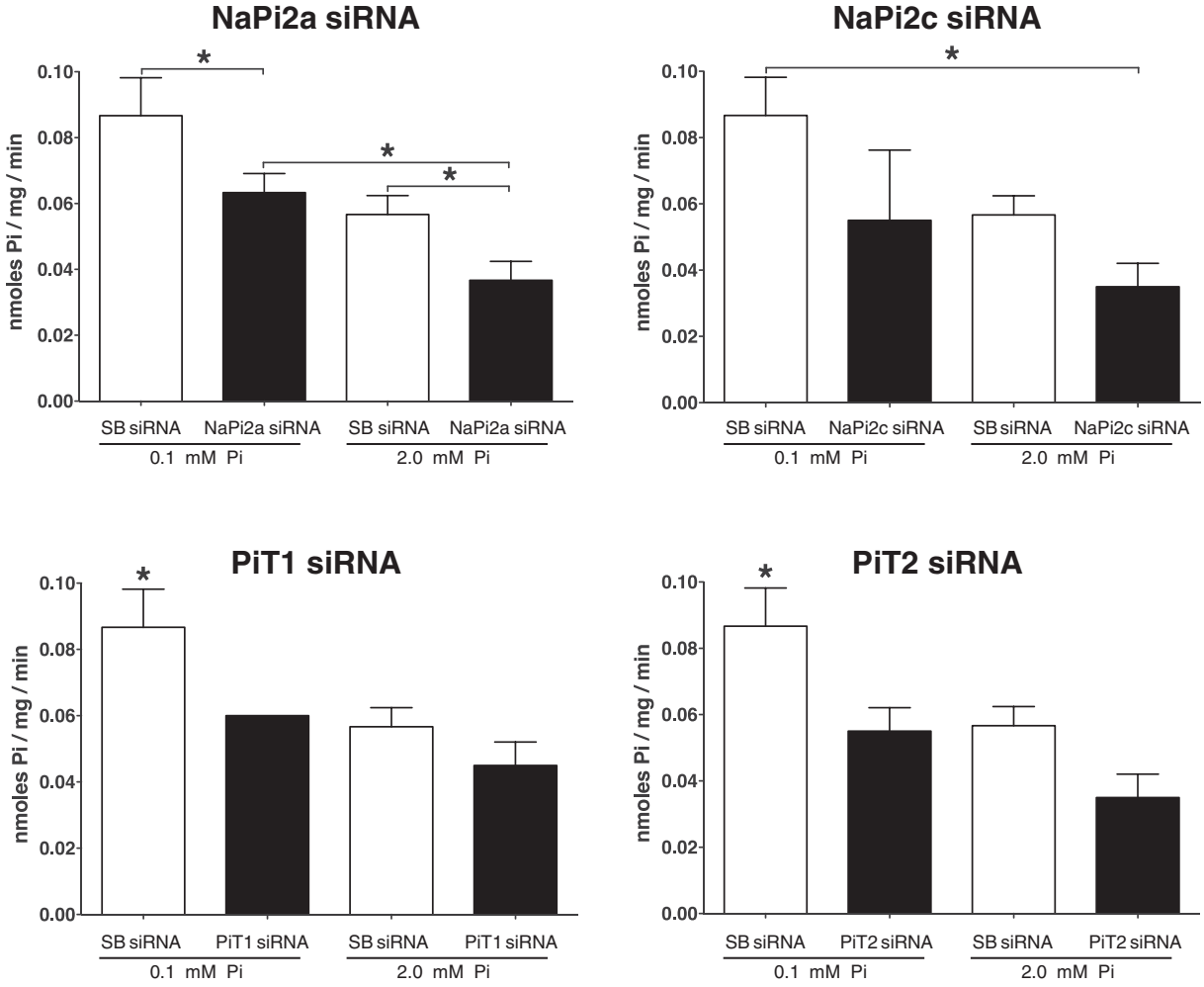

FIGURE 8 Effects of NaPiIIa, NaPiIIc, PiT1 and PiT2 RNA interference on adaptation of P_i transport to low and high P_i concentrations in OK cells after 72 h of siRNA transfections at pH 7.4. Abbreviation: SB, scrambled siRNA. Asterisks in the top two panels indicate significantly different means by ANOVA ($P < 0.05$). Asterisks in the PiT1 and PiT2 panels indicate significant differences from all other conditions

(Fenollar-Ferrer et al., 2014). Some previous TMDs have been replaced by hairpins and intramembrane loops, while the last two TMDs are maintained, but they are not a part of the repeated core. The function of these two last TMDs is still unclear, but the intracellular cytosolic domain anchors the protein to the cytoskeleton through PDZ domain proteins.

Based on the amino acid sequences, we prepared polyclonal antibodies for the new transporters, but none of them provided specific and reliable signals in the western blot analysis. The determination of NaPiIIc from OK cells has been reported previously using an antibody raised against a peptide corresponding to the C-terminus of NaPiIIc from *M. domestica* (Ito et al., 2010). The sequences of the C-ends of both opossum NaPiIIc are most probably very similar or even identical. Nevertheless, because the C-terminus of the American opossum was missing in our 3′-RACE and because we also lacked antibodies against PT1 and PiT2, we decided to homogenize the results and focus on the functional and RNA regulation of all four P_i transporters. A striking characteristic of the OK culture is the great variability as a function of the proliferation state and confluency (Figure 4). The more confluent the cells are, the higher the expression of type II, whereas the converse is true for type III, in which expression is lower to the extent that confluency is greater. In confluent OK cells, the expression of PiT2 is negligible, and in highly proliferating cells the expressions of NaPiIIa and NaPiIIc are extremely low. The characteristics of P_i transport in confluent OK cells are typical of the proximal tubule, i.e. type II P_i transport, meaning that it is increased by an alkaline pH and is inhibited by PFA (Figure 3). Only at pH 6.0, when the monovalent P_i species is most abundant, is type III P_i transport revealed, which is resistant to PFA inhibition (Figure 3b). At this confluent state, NaPiIIa and NaPiIIc are most abundant, but PiT1 is also significantly expressed (Figure 4), which is consistent with the results in both figures; transport characteristics and RNA expression.

In addition to NaPiIIa (e.g. Markovich et al., 1995; Pfister et al., 1998; Thomas, Wagner, Biber, & Hernando, 2016; Villa-Bellosta & Sorribas, 2009), adaptation to a low P_i concentration in a culture medium also affects NaPiIIc RNA in OK cells (Figure 6). In the case of NaPiIIa (Markovich et al., 1995) and most probably regarding NaPiIIc, the increase in mRNA seems to be attributable to an increased stability of RNA rather than increased transcription. We have also quantified the abundance of NaPiIIc mRNA after treatment with T_3, a hormone

known to increase the abundance of NaPiIIa transcriptionally in OK cells and in rats (Alcalde et al., 1999; Sorribas et al., 1995). The NaPiIIa RNA increased as expected (Figure 6c), and the increase was similar for NaPiIIc but was absent in the case of PiT1 and PiT2.

With respect to the molecular mechanisms of chronic adaptation to a low P_i concentration in culture medium, previous transport assays had been performed at pH 7.4, and only the RNA of NaPiIIa (NaPi4) was evaluated (e.g. Markovich et al., 1995). By inhibiting transcription with actinomycin D, we have, in part, confirmed those previous results. NaPiIIc and both PiT1 and PiT2 (mainly) are very sensitive to actinomycin D treatment, and after 24 h their RNA levels drop dramatically and prevent P_i transport adaptation when measured at pH 6.0. These results strongly suggest that the half-life of NaPiIIa RNA is the longest of all four transcripts.

Using siRNA, these conclusions were confirmed only in part. The main problem with this technology is that, to reach acceptable transfection efficiency, the OK cell culture needs to be non-confluent, and the expression of P_i transporters will differ considerably from the time of confluence, as we have shown. Moreover, not only does siRNA prevent the initiation of nascent RNAs, but the final and steady-state abundance of the specific transcripts is also affected. Taking these limitations into account, the inhibition of the specific transcripts revealed that P_i transport was not affected by PiT1 siRNA; that PiT2 interference moderately affected P_i transport, despite the low expression; and that NaPiIIa and NaPiIIc siRNAs strongly affected P_i transport in a similar, although not completely (Figure 7). The non-effect by PiT1 siRNA could be explained by the long half-life of the protein, an issue that can be addressed only when a good antibody is obtained. Also, PiT1 has additional functions, such as proliferation/apoptosis (Beck et al., 2009; Kongsfelt, Byskov, Pedersen, & Pedersen, 2014) and P_i sensing (Bon et al., 2018; Salaün et al., 2002), and at least in vascular smooth muscle cells, the protein is also expressed intracellularly (Villa-Bellosta, Levi, & Sorribas, 2009a).

The effects of siRNAs were also studied regarding the ability of cells to adapt to the concentration of P_i in the culture medium. The siRNA treatment affected the process of adaptation in all four cases, but with important differences (Figure 8). NaPiIIa siRNA prevents adaptation to 0.1 mmol l^{-1} of P_i when compared with scrambled siRNA-treated cells incubated with 2 mmol l^{-1} P_i, but when compared with NaPiIIa siRNA-treated cells incubated with 2 mmol l^{-1} P_i, adaptation persists. The effect of siRNA on NaPiIIc was similar but more modest. The PiT1 and PiT2 siRNAs also completely prevented the adaptation of P_i transport to a low P_i concentration. Given that the expressions of both transporters are very low, a likely explanation is that these transporters have other functions in addition to P_i transport, as indicated above.

To summarize, confluent OK cells show a combination of type II and type III P_i transport, with major expression of NaPiIIa and NaPiIIc, minor expression of PiT1 and negligible expression of PiT2. NaPiIIa, NaPiIIc, PiT1 and PiT2 are all involved in the handling of P_i by these cells, but they seem to have very different roles at the basal transport rate and during increased transport induced by a low P_i concentration.

ACKNOWLEDGEMENTS

The authors would like to thank Professor Eleanor Lederer (University of Louisville School of Medicine, KY, USA) for donating the only functional antibody against NaPiIIa (NaPi4) from OK cells.

AUTHOR CONTRIBUTIONS

All the experiments were performed at the Department of Toxicology, University of Zaragoza (Spain). M.L. and V.S. contributed to the conception and design of the work. N.G. and Y.A.C. contributed to the acquisition of data, and N.G., Y.A.C. and V.S. contributed to the analysis and interpretation of the data. V.S. drafted the manuscript, and N.G., Y.A.C., M.L. and V.S. revised it critically for important intellectual content. All authors approved the final version of the manuscript and agree to be accountable for all aspects of the work in ensuring that questions related to the accuracy or integrity of any part of the work are appropriately investigated and resolved. All persons designated as authors qualify for authorship, and all those who qualify for authorship are listed.

COMPETING INTERESTS

None declared.

ORCID

Yupanqui A. Caldas https://orcid.org/0000-0002-4666-3155
Víctor Sorribas https://orcid.org/0000-0003-3457-323X

REFERENCES

Alcalde, A. I., Sarasa, M., Raldúa, D., Aramayona, J., Morales, R., Biber, J., … Sorribas, V. (1999). Role of thyroid hormone in regulation of renal phosphate transport in young and aged rats. *Endocrinology*, *140*, 1544–1551. https://doi.org/10.1210/endo.140.4.6658

Beck, L, Leroy, C., Salaün, C., Margall-Ducos, G., Desdouets, C., & Friedlander, G. (2009). Identification of a novel function of PiT1 critical for cell proliferation and independent of its phosphate transport activity. *Journal of Biological Chemistry*, *284*, 31363–31374. https://doi.org/10.1074/jbc.M109.053132

Biber, J., Hernando, N., & Forster, I. (2013). Phosphate transporters and their function. *Annual Review of Physiology*, *75*, 535–550. https://doi.org/10.1146/annurev-physiol-030212-183748

Bon N, Couasnay G, Bourgine A, Sourice S, Beck-Cormier S, Guicheux J, & Beck L (2018). Phosphate (P_i)-regulated heterodimerization of the high-affinity sodium-dependent P_i transporters PiT1/Slc20a1 and PiT2/Slc20a2 underlies extracellular P_i sensing independently of P_i uptake. *Journal of Biological Chemistry*, *293*, 2102–2114.

Bøttger, P., & Pedersen, L. (2011). Mapping of the minimal inorganic phosphate transporting unit of human PiT2 suggests a structure universal to PiT-related proteins from all kingdoms of life. *BMC Biochemistry*, *12*, 21. https://doi.org/10.1186/1471-2091-12-21

Candeal, E., Caldas, Y. A., Guillén, N., Levi, M., & Sorribas, V. (2017). Intestinal phosphate absorption is mediated by multiple transport systems in rats. *American Journal of Physiology. Gastrointestinal and Liver Physiology*, *312*, G355–G366. https://doi.org/10.1152/ajpgi.00244.2016

Chang, A. R., & Anderson, C. (2017). Dietary phosphorus intake and the kidney. *Annual Review of Nutrition*, *37*, 321–346. https://doi.org/10.1146/annurev-nutr-071816-064607

Fenollar-Ferrer, C., Patti, M., Knöpfel, T., Werner, A., Forster, I. C., & Forrest, L.R. (2014). Structural fold and binding sites of the human Na^+-phosphate cotransporter NaPi-II. *Biophysical Journal*, *106*, 1268–1279. https://doi.org/10.1016/j.bpj.2014.01.043

Forster, I. C., Hernando, N., Biber, J., & Murer, H. (2012). Phosphate transport kinetics and structure-function relationships of SLC34 and SLC20 proteins. *Current Topics in Membranes*, *70*, 313–356. https://doi.org/10.1016/B978-0-12-394316-3.00010-7

Forster, I. C., Hernando, N., Biber, J., & Murer, H. (2013). Phosphate transporters of the SLC20 and SLC34 families. *Molecular Aspects of Medicine*, *34*, 386–395. https://doi.org/10.1016/j.mam.2012.07.007

Forster, I., & Werner, A. (2018). SLC34. In S. Choi (Ed.), *Encyclopedia of signaling molecules*, pp. 5013–5022. Cham: Springer. https://doi.org/10.1007/978-3-319-67199-4_101997

Hartmann, C. M., Wagner, C. A., Busch, A. E., Markovich, D., Biber, J., Lang, F., & Murer H. (1995). Transport characteristics of a murine renal Na/Pi-cotransporter. *Pflügers Archiv*, *430*, 830–836.

Ito, M., Sakurai, A., Hayashi, K., Ohi, A., Kangawa, N., Nishiyama, T., … Miyamoto, K. (2010). An apical expression signal of the renal type IIc Na^+-dependent phosphate cotransporter in renal epithelial cells. *American Journal of Physiology. Renal Physiology*, *299*, F243–F254. https://doi.org/10.1152/ajprenal.00189.2009.

Komaba, H., & Fukagawa, M. (2016). Phosphate—A poison for humans? *Kidney International*, *90*, 753–763. https://doi.org/10.1016/j.kint.2016.03.039

Kongsfelt, I. B., Byskov, K., Pedersen, L. E., & Pedersen, L. (2014). High levels of the type III inorganic phosphate transporter PiT1 (SLC20A1) can confer faster cell adhesion. *Experimental Cell Research*, *326*, 57–67. https://doi.org/10.1016/j.yexcr.2014.05.014

Koyama, H., Goodpasture, C., Miller, M. M., Teplitz, R. L., & Riggs, A. D. (1978). Establishment and characterization of a cell line from the American opossum (*Didelphys virginiana*). *In Vitro*, *14*, 239–246.

Lederer, E. D., Sohi, S. S., Mathiesen, J. M., & Klein, J. B. (1998). Regulation of expression of type II sodium-phosphate cotransporters by protein kinases A and C. *American Journal of Physiology. Renal Physiology*, *275*, F270–F277. https://doi.org/10.1152/ajprenal.1998.275.2.F270

Malmström, K., & Murer, H. (1986). Parathyroid hormone inhibits phosphate transport in OK cells but not in LLC-PK1 and JTC-12.P3 cells. *American Journal of Physiology. Cell Physiology*, *251*, C23–C31. https://doi.org/10.1152/ajpcell.1986.251.1.C23

Mancusso, R., Gregorio, G. G., Liu, Q., & Wang, D. N. (2012). Structure and mechanism of a bacterial sodium-dependent dicarboxylate transporter. *Nature*, *491*, 622–626. https://doi.org/10.1038/nature11542

Markovich, D., Verri, T., Sorribas, V., Forgo, J., Biber, J., & Murer H. (1995). Regulation of opossum kidney (OK) cell Na/Pi cotransport by Pi deprivation involves mRNA stability. *Pflügers Archiv*, *430*, 459–463. https://doi.org/10.1007/BF00373881

Marks, J., Debnam, E. S., & Unwin, R. J. (2010). Phosphate homeostasis and the renal-gastrointestinal axis. *American Journal of Physiology. Renal Physiology*, *299*, F285–F296. https://doi.org/10.1152/ajprenal.00508.2009

Patti, M., Ghezzi, C., & Forster, I. C. (2013). Conferring electrogenicity to the electroneutral phosphate cotransporter NaPi-IIc (SLC34A3) reveals an internal cation release step. *Pflügers Archiv*, *465*, 1261–1279. https://doi.org/10.1007/s00424-013-1261-9

Pfister, M. F., Hilfiker, H., Forgo, J., Lederer, E., Biber, J., & Murer, H. (1998). Cellular mechanisms involved in the acute adaptation of OK cell Na/Pi-cotransport to high- or low-Pi medium. *Pflügers Archiv*, *435*, 713–719. https://doi.org/10.1007/s004240050573

Ravera, S., Murer, H., & Forster, I. C. (2013). An externally accessible linker region in the sodium-coupled phosphate transporter PiT-1 (SLC20A1) is important for transport function. *Cellular Physiology and Biochemistry*, *32*, 187–199. https://doi.org/10.1159/000350135

Salaün, C., Gyan, E., Rodrigues, P., & Heard, J. M. (2002). Pit2 assemblies at the cell surface are modulated by extracellular inorganic phosphate concentration. *Journal of Virology*, *76*, 4304–4311. https://doi.org/10.1128/JVI.76.9.4304-4311.200.

Sorribas, V., Markovich, D., Hayes, G., Stange, G., Forgo, J., Biber, J., & Murer, H. (1994). Cloning of a Na/Pi cotransporter from opossum kidney cells. *Journal of Biological Chemistry*, *269*, 6615–6621.

Sorribas, V., Markovich, D., Verri, T., Biber, J., & Murer, H. (1995). Thyroid hormone stimulation of Na/Pi-cotransport in opossum kidney cells. *Pflügers Archiv*, *431*, 266–271. https://doi.org/10.1007/BF00410200

Sorribas, V (2018). SLC20. In S. Choi (Ed.), *Encyclopedia of signaling molecules*, pp. 4987–4994. Cham: Springer. https://doi.org/10.1007/978-3-319-67199-4_101880

Thomas, L., Wagner, C. A., Biber, J., & Hernando, N. (2016). Adaptation of opossum kidney cells to luminal phosphate: Effects of phosphonoformic acid and kinase inhibitors. *Kidney & Blood Pressure Research*, *41*, 298–310. https://doi.org/10.1159/000443432

Villa-Bellosta, R., Barac-Nieto, M., Breusegem, S. Y., Barry, N. P., Levi, M., & Sorribas, V. (2008). Interactions of the growth-related, type IIc renal sodium/phosphate cotransporter with PDZ proteins. *Kidney International*, *73*, 456–464. https://doi.org/10.1038/sj.ki.5002703

Villa-Bellosta, R., Levi, M., & Sorribas, V. (2009a). Vascular smooth muscle cell calcification and SLC20 inorganic phosphate transporters: Effects of PDGF, TNF-α, and Pi. *Pflügers Archiv*, *458*, 1151–1161. https://doi.org/10.1007/s00424-009-0688-5

Villa-Bellosta, R., Ravera, S., Sorribas, V., Stange, G., Levi, M., Murer, H., … & Forster IC. (2009b). The Na^+-P_i cotransporter PiT-2 (SLC20A2) is expressed in the apical membrane of rat renal proximal tubules and regulated by dietary P_i. *American Journal of Physiology. Renal Physiology*, *296*, F691–F699. https://doi.org/10.1152/ajprenal.90623.2008

Villa-Bellosta, R., & Sorribas, V. (2009). Different effects of arsenate and phosphonoformate on P_i transport adaptation in opossum kidney cells. *American Journal of Physiology. Cell Physiology*, *297*, C516–C525. https://doi.org/10.1152/ajpcell.00186.2009

How to cite this article: Guillén N, Caldas YA, Levi M, Sorribas V. Identification and expression analysis of type II and type III P_i transporters in the opossum kidney cell line. *Exp Physiol*. 2019;104:149–161. https://doi.org/10.1113/EP087217